

A universal origin for secondary relaxations in supercooled liquids and structural glasses

Jacob D. Stevenson

*Department of Physics and Department of Chemistry and Biochemistry,
Center for Theoretical Biological Physics, University of California, San Diego, La Jolla, CA 92093*

Peter G. Wolynes

*Department of Physics and Department of Chemistry and Biochemistry,
Center for Theoretical Biological Physics, University of California, San Diego, La Jolla, CA 92093 and
e-mail: pwolynes@ucsd.edu
(Dated: February 21, 2024)*

Nearly all glass forming liquids display secondary relaxations, dynamical modes seemingly distinct from the primary alpha relaxations. We show that accounting for driving force fluctuations and the diversity of reconfiguring shapes in the random first order transition theory yields a low free energy tail on the activation barrier distribution which shares many of the features ascribed to secondary relaxations. While primary relaxation takes place through activated events involving compact regions, secondary relaxation corresponding to the tail is governed by more ramified, string-like, or percolation-like clusters of particles. These secondary relaxations merge with the primary relaxation peak becoming dominant near the dynamical crossover temperature T_c , where they smooth the transition between continuous dynamics described by mode-coupling theory and activated events.

Diversity, a key feature of glassy systems, is most apparent in their relaxation properties. Dielectric, mechanical and calorimetric responses of supercooled liquids are not single exponentials in time, but manifest a distribution of relaxation times. The typical relaxation time grows upon cooling the liquid until it exceeds the preparation time, yielding a non-equilibrium glass, which can still relax but in an age dependent fashion. In addition to the main relaxations that are responsible for the glass transition, supercooled liquids and structural glasses exhibit faster motions, some distinct enough in time scale from the typical relaxation to be called “secondary” relaxation processes[1, 2, 3, 4, 5]. These faster motions account for only a fraction of the relaxation amplitude in the liquid but become dominant features in the relaxation of otherwise frozen glass, where they are important to the mechanical properties. These secondary relaxation processes in the solvation shell of proteins are also prominent in protein dynamics[6].

The phenomenology of secondary relaxation has been much discussed but, owing especially to the problem of how to subtract the main peak, the patterns observed seem to be more complex and system specific than those for the main glassy relaxation. Some of the secondary relaxation motions are, doubtless, chemically specific, occurring on the shortest length scales. Nevertheless the presence of secondary relaxation in glassy systems is nearly universal[7]. In this paper we will show how secondary relaxations naturally arise in the random first order transition (RFOT) theory of glasses[8] and are predicted to scale in intensity and frequency in a manner consistent with observation.

The RFOT theory is based on the notion that there is a diversity of locally frozen free energy minima that

can inter-convert via activated transitions. The inter-conversions are driven by an extensive configurational entropy. RFOT theory accounts for the well known correlations between the primary relaxation time scale in supercooled liquids and thermodynamics[9, 10] as well as the aging behavior in the glassy state[11]. By taking account of local fluctuations in the driving force, RFOT theory also gives a good account of the breadth of the rate distribution of the main relaxation[12, 13]. Here we will argue that RFOT theory suggests, universally, a secondary relaxation also will appear and that its intensity and shape depends on the configurational thermodynamics of the liquid. This relaxation corresponds with the low free energy tail of the activation barrier distribution. The distinct character of this tail comes about because the geometry of the reconfiguring regions for low barrier transitions is different from that of those rearranging regions responsible for the main relaxation. Near to the laboratory T_g , the primary relaxation process involves reconfiguring a rather compact cluster, but the reconfiguring clusters become more ramified as the temperature is raised and eventually resembling percolation clusters or strings near the dynamical crossover to mode coupling behavior, identified with the onset of non-activated motions[14]. Reconfiguration events of the more extended type are more susceptible to fluctuations in the local driving force, even away from the crossover. These ramified or “stringy” reconfiguration events thus dominate the low barrier tail of the activation energy distribution.

When the shape distribution of reconfiguration processes is accounted for, a simple statistical computation shows that a two peaked distribution of barriers can arise. This calculation motivates a more explicit but approxi-

mate theory that gives analytical expressions for the distribution of relaxation times in the tail. In keeping with experiment, the theory predicts the secondary relaxation motions are actually most numerous near the crossover, but of course, merge in frequency with the main relaxation peak in time scale also at that crossover. Furthermore the relaxation time distribution for secondary relaxations is predicted to be described by an asymptotic power law. The theory is easily extended to the aging regime where these secondary relaxations can dominate the rearranging motions.

In RFOT theory, above the glass transition temperature, the entropic advantage of exploring phase space, manifested as a driving force for reconfiguration, is balanced by a mismatch energy at the interface between adjacent metastable states. For a flat interface in the deeply supercooled regime the mismatch energy can be described as a surface tension that can be estimated from the entropy cost of localizing a bead[9, 15], giving a surface tension $\sigma_0 = (3/4)k_B T r_0^{-2} \ln[1/(d_L^2 \pi e)]$ where d_L is the Lindemann length, the magnitude of particle fluctuations necessary to break up a solid structure, and is nearly universally a tenth of the inter-particle spacing, ($d_L = 0.1r_0$). The free energy profile for reconfiguration events resembles nucleation theory at first order transitions but is conceptually quite distinct. Following Stevenson-Schmalian-Wolynes (SSW)[14] the free energy cost of an N particle cluster with surface area Σ making a structural transition to a new metastable state may be written

$$F(N, \Sigma) = \Sigma \sigma_0 - N k_B T s_c - k_B T \ln \Omega(N, \Sigma) - \sum_{\text{particles}} \delta \tilde{f} \quad (1)$$

A key element of the free energy profile is the shape entropy $k_B \log \Omega(N, \Sigma)$ which accounts for the number of distinct ways to construct a cluster of N particles having surface area Σ . At one extreme are compact, nearly spherical objects with shape entropy close to zero. While objects such as percolation clusters or stringy chains have surface area and shape entropy both of which grow linearly with N . The last term of equation 1 accounts for the inherent spatial fluctuations in the disordered glassy system that give fluctuations in the driving force. We presently ignore local fluctuations in the surface mismatch free energy, but their inclusion would not qualitatively alter the results[13, 16, 17]. We simplify by assuming uncorrelated disorder, so each particle joining the reconfiguration event is given a random energy, $\delta \tilde{f}$, drawn from a distribution of width $\delta \tilde{f}$. The r.m.s. magnitude of the driving force fluctuations above T_g follows from the configurational heat capacity through the relation $\delta \tilde{f} \approx T \sqrt{\Delta C_p} k_B$, a result expected for large enough regions. We will assume no correlations for simplicity, but they can be included.

For nearly spherical reconfiguring regions forming compact clusters the shape entropy is very small and the mismatch free energy is $\sigma_0 4\pi (3N/(4\pi \rho_0))^{\theta/3}$ with $\theta = 2$ if fluctuations are small. In disordered systems the mismatch free energies grow with exponent θ generally less than 2 reflecting preferred growth in regions of favorable energetics and the large number of metastable states which can wet the interface and reduce the effective surface tension. A renormalization group treatment of the wetting effect[15] suggests that $\theta = 3/2$ in the vicinity of an ideal glass transition. Incomplete wetting giving strictly $\theta = 2$ only asymptotically would not change the numerics of the present theory much. Whether complete wetting occurs for supercooled liquids under laboratory conditions is still debated[17, 18, 19]. The free energy profile describing reconfiguration events restricted to compact clusters becomes, then, $F_{\text{compact}}(N) = \sigma_0 4\pi (3N/(4\pi \rho_0))^{\theta/3} - N T s_c$. The minimum number of particles participating in a reconfiguration event is determined by finding where the free energy profile crosses zero. For $\theta = 3/2$ the activation free energy barrier is inversely proportional to the configurational entropy, leading to the Adam-Gibbs[20] relation for the most probable relaxation time $F_{\alpha}^{\ddagger}/k_B T \sim \ln \tau_{\alpha}/\tau_0 \sim s_c^{-1}$. Adding fluctuations to the profile of compact reconfiguration events yields an approximate Gaussian distribution of barriers with width scaling as $\sqrt{N^{\ddagger}} \delta \tilde{f}$. Xia and Wolynes[12], and more explicitly Bhattacharyya et al.[21], have shown that, with the inclusion of facilitation effects, the resulting barrier distribution accounts for the stretching of the main relaxation process and yields good estimates for how the stretching exponent varies with liquid fragility.

Restricting the reconfiguration events to stringy clusters (using percolation clusters gives very similar results), gives a free energy profile linear in the number of particles reconfigured, save for the minimum cost F_{in} to begin to reconfigure a region:

$$F_{\text{string}}(N) = -N T (s_c - s_c^{\text{string}}) + F_{\text{in}}. \quad (2)$$

The critical “entropy” is given by $T s_c^{\text{string}} = v_{\text{int}}(z - 2) - k_B T \ln(z - 5) \approx 1.13 k_B T$. This is the difference between the surface energy written in terms of the coordination number of the random close packed lattice $z \approx 12$ (v_{int} is the surface tension per nearest neighbor) and the shape entropy including excluded volume effects[22]. If a bead can individually reconfigure then the cost to begin to reconfigure is $F_{\text{in}} = z v_{\text{int}} - T s_c \approx 2.5 - 2.9 k_B T$. If two must be moved then $F_{\text{in}} \approx 6.1 k_B T$. The continuous form of the surface mismatch energy gives a somewhat higher value when applied to these small regions, giving $F_{\text{in}}^{\text{continuous}} = r_0^2 \sigma_0 4\pi (3/(4\pi))^{\theta/3} - T s_c \approx 10.5 k_B T$ for a one particle reconfiguration. The remarkably simple free energy profile of equation 2 monotonically increases, so that below T_{string} (defined by $s_c(T_{\text{string}}) = s_c^{\text{string}}$) reconfiguration via pure stringy objects is impossible. Above

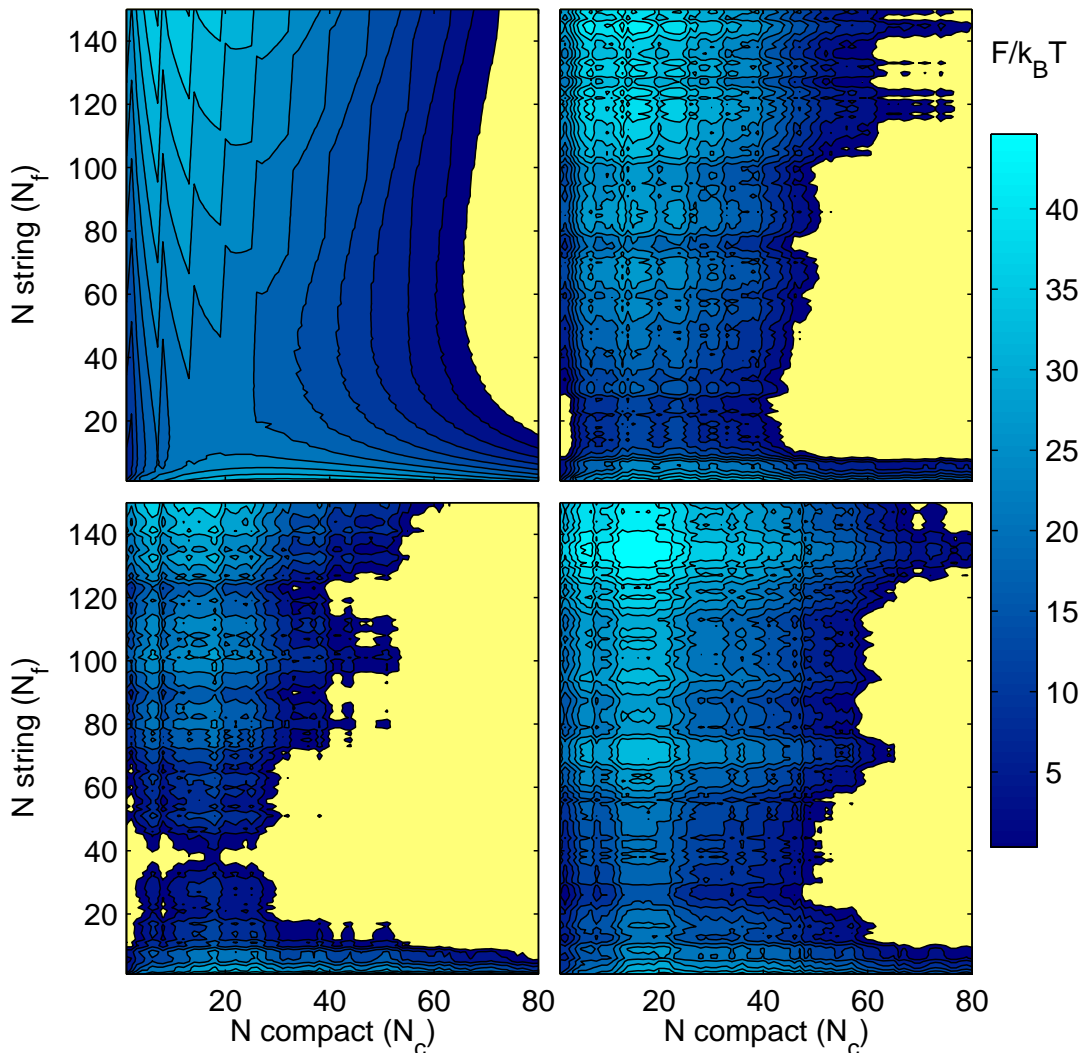


FIG. 1: The two dimensional free energy profile describing cooperative relaxation as a function of the number of compact particles N_c and the number of stringy particles N_f in the reconfiguring region. The transition state separating the unreconfigured state ($N_c = N_f = 0$) with the final stable state (colored yellow in the figure) determines the free energy barrier to reconfiguration. The upper left panel gives the profile ($s_c = 1.0k_B$) in the absence of fluctuations while the others demonstrate three possible realizations of fluctuations for a relatively strong liquid, a liquid having $\Delta C_P \approx 1k_B$ per bead. The fluctuations for the two dimensional profile are implemented as cumulative sums of local fluctuations in both N_c and N_f . For the situation described in the bottom right panel compact reconfiguration is required to overcome the free energy barrier. For the two other realizations the fluctuations are such that stable (yellow) regions exist along the vertical axis, meaning string-like reconfiguration is possible. These stringy clusters, stabilized by fluctuations, account for the secondary relaxation.

T_{string} the same process can occur with very small free energy barrier, having only to overcome F_{in} . Thus T_{string} signals the crossover from dynamics dominated by activated events to dynamics dominated by non-activated processes. Interestingly, this crossover is mathematically analogous to the Hagedorn transition of particle theory[23]. The predicted constant value of s_c^{string} is confirmed experimentally[14]. In contrast to the situation for compact reconfiguration, driving force fluctuations dramatically alter the picture of stringy relaxation. With driving force fluctuations a lucky sequence of fluctuations

can easily push the nominally linearly increasing free energy profile to cross zero, so strings can be active below T_c .

SSW[14] introduced a crude model to estimate the shape entropy and surface area of the range of shapes between the extremes. This “fuzzy sphere” model, consists of a compact center of N_c particles with a stringy halo of N_f particles. With this interpolative model T_g the preferred shape of a reconfiguring region is largely compact, while the relevant regions become more ramified close to T_c . Fluctuations, aggregated cumulatively in

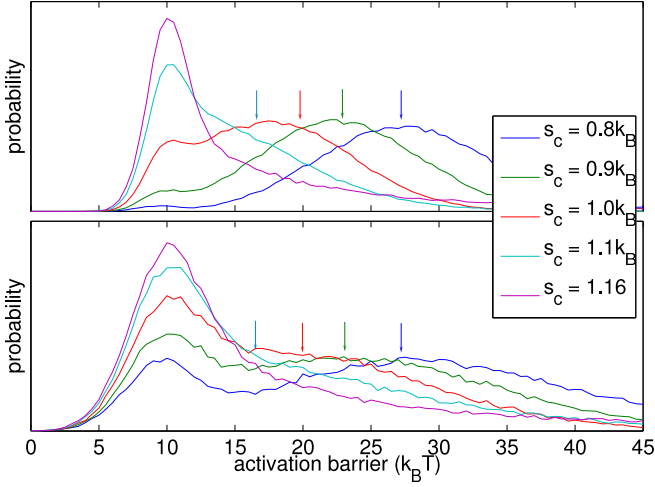


FIG. 2: Probability distribution of free energy barriers governing relaxation events in supercooled liquids. Different curves represent different temperatures, increasing from near the glass transition temperature to near the dynamical crossover temperature. The arrows indicate the typical relaxation time predicted from the fuzzy sphere model without fluctuations. The dashed line gives the distribution of free energy barriers for a liquid just above the dynamical crossover temperature where primary relaxations disappear leaving only the secondary process. The top panel corresponds to a rather strong liquid with small fluctuations, $\Delta C_P \approx 1 k_B$ per bead — a material similar to GeO_2 . The bottom panel corresponds to a fragile liquid with larger fluctuations, $\Delta C_P = 3 k_B$ per bead — a material similar to orthoterphenyl. Secondary relaxations, i.e. relaxation events using string-like rearranging regions, increase in prominence as the temperature is increased, becoming the dominant process near the dynamical crossover temperature where the two peaks merge. The units of the activation energy are given in $k_B T$, which assumes a mismatch penalty primarily entropic in nature, $\sigma_0 \sim k_B T$. An energetic mismatch penalty, $\sigma_0 \sim k_B T_K$, would lead to Arrhenius behavior for the secondary relaxation process, as the distribution is peaked around the minimum free energy to initiate a stringy reconfiguration, F_{in} . In this calculation we have used the continuous approximation of F_{in} shown in the text. The facilitation phenomenon, as described by Xia and Wolynes[12] and by Bhattacharya et al.[21] but not accounted for here, would shift weight from the largest free energies to the center of the primary peak, raising the overall height of the primary peak relative to the secondary peak.

the compact core yielding a variance proportional to N_c , and cumulatively in the stringy halo yielding a variance proportional to N_f , modify the SSW two dimensional free energy landscape. The local free energy plots for several realizations of such accumulated fluctuations, assumed to have Gaussian statistics, are given in figure 1. For some realizations compact reconfiguration will still be required to overcome the free energy barrier, but for other realizations the fluctuations are such that the free energy cost for reconfiguration crosses zero along the N_f axis (shown in the figure in yellow) so the region is able

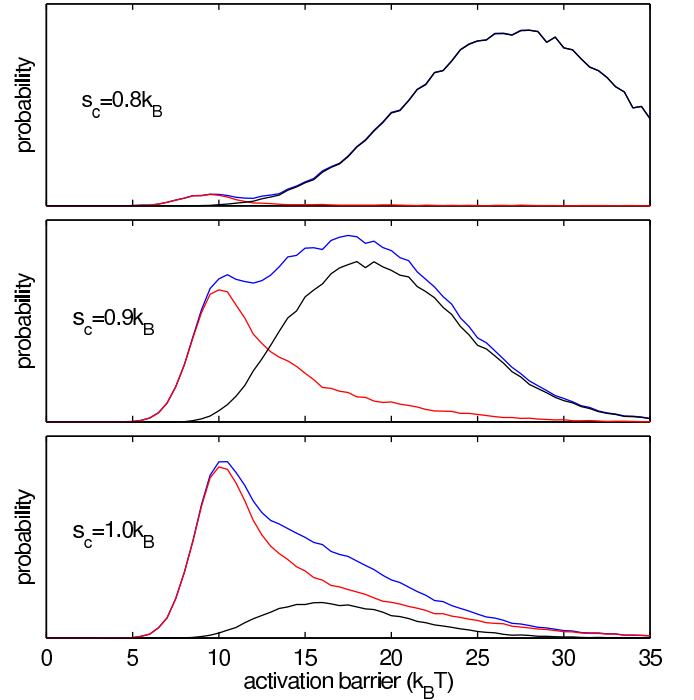


FIG. 3: Distribution of free energy barriers for a strong liquid ($\Delta C_P \approx 1 k_B$ per bead) separated into the contribution from secondary relaxations (red curves), corresponding to string-like reconfiguration as in panels b and c of figure 1, and primary relaxations (black curves), corresponding to compact reconfigurations. The full distributions are given for comparison (blue curves). The separation of the curves makes clear that as the dynamical crossover temperature is approached the primary relaxation becomes subordinate to the secondary relaxation.

to relax via a string-like reconfiguration event. These stringy rearranging clusters, stabilized by disorder, we argue, are key contributors to the secondary relaxation process. The statistics of the stable reconfiguration paths with lowest free energy barrier are summarized in figure 2 with barrier distributions for two different values of δf corresponding to a strong and a fragile liquid. We can disaggregate these distributions into the parts due, separately, to the compact events (“primary”) and to the string-like fluctuation induced events (“secondary”). These distributions are shown in figures 3 and 4. At temperatures near T_g compact primary relaxations dominate reconfiguration, but as the temperature increases, fluctuations are able to stabilize string-like reconfiguration more easily and the secondary relaxations increases in prominence. At the same time, with increasing temperature, the primary relaxation peak shifts to lower free energy barriers, making it difficult to distinguish between the two contributions. As T_c is approached and crossed, the primary and secondary peaks merge with string-like reconfiguration clusters becoming the dominant mode of relaxation. For fragile liquids, i.e. liquids with larger con-

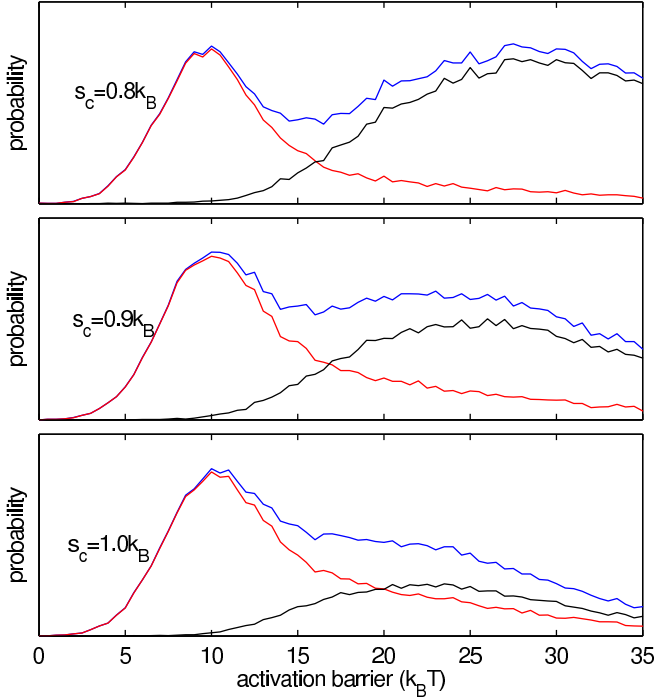


FIG. 4: The corresponding results to those of figure 3 but for a fragile liquid, one with $\Delta C_P \approx 3k_B$ per bead.

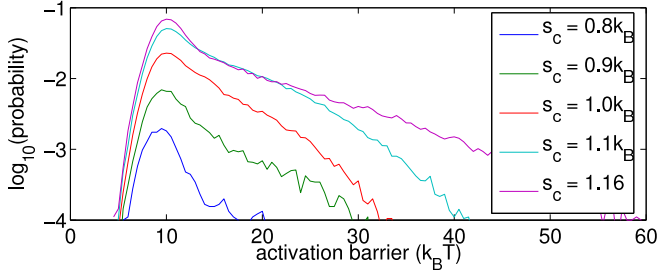


FIG. 5: Distribution of free energy barriers for the secondary relaxation process from the statistical sampling of the fuzzy sphere model with fluctuations. The data correspond to a strong liquid ($\Delta C_P \approx 1$) and show that at higher temperatures (larger configurational entropies) the distribution decays more slowly. This leads to wider activation energy distributions, matching the expectations of the analytical calculations.

figural entropy fluctuations[10], the secondary relaxation peak is generally more important than for strong liquids. Both peaks are broader and begin to merge at lower temperatures for the more fragile liquids. Because facilitation effects are not explicitly accounted for (these would mostly affect the higher barriers) it is not easy to directly compare these predicted distributions with quantitative precision to experiment. In addition, the number of reconfiguring particles in the two peaks is different, so their contributions to the measured amplitudes are different as well. Nevertheless, the predicted magnitude of the secondary relaxation peak, as compared to the primary

peak, seems to be somewhat larger than experiments apparently show. This disparity is more pronounced for fragile materials. The assumptions in the fuzzy sphere model, and especially the assumption of uncorrelated disorder, apparently overestimate the influence of the fluctuations, which are probably (anti-) correlated for the most fragile systems.

The barrier distribution for reconfiguration events that take an ideal stringy form can be explicitly calculated. A similar analysis to the string case can be applied to reconfiguration via percolation clusters but with somewhat different numerical constants in the relation of the free energy profile to N . This analytic calculation resembles that of Plotkin and Wolynes for the “buffing” of protein folding energy landscapes[24]. The key to the calculation of $\Gamma(F^\ddagger)$, the distribution of free energy barriers for events with less than N_{\max} displaced atoms, lies in mapping the problem onto a random walk, or a diffusion process in free energy space. Going to the limit of continuous number of particles we may write a stochastic differential equation for the free energy profile $dF/dN = dF_{\text{string}}/dN + \delta\tilde{f}$. The principal quantity to compute is $G(N, F^\ddagger; F_{\text{in}})$, the probability that a reconfiguration path of N particles has free energy F if the cost to initiate the reconfiguration event is F_{in} . The evolution of G , that follows from the stochastic profile, is described by a diffusion equation with drift subject to absorbing boundary conditions at both $F = 0$ and $F = F^\ddagger$. These boundary conditions permit the calculation of the distribution of free energy barriers by keeping track of the maximum excursion of the random walk.

$$\frac{\partial G}{\partial N} + \phi \frac{\partial G}{\partial F} = \frac{1}{2} \delta f^2 \frac{\partial^2 G}{\partial F^2}, \quad (3)$$

The slope of the mean free energy profile $\phi = T(s_c^{\text{string}} - s_c)$ depends simply on the proximity to the string transition. ϕ is a string tension reflecting the free energy cost of lengthening a string. The probability density for the maximum excursion of F is then

$$\Gamma(F^\ddagger) = -\frac{\partial}{\partial F^\ddagger} \int_0^{N_{\max}} dN \left\langle \frac{\delta f^2}{2} \frac{\partial G}{\partial F} \right|_{F=0} \Big|_{0 < F_{\text{in}} < F^\ddagger}. \quad (4)$$

The average $\langle \cdot \rangle_{0 < F_{\text{in}} < F^\ddagger}$ is present to integrate over the fluctuations in the free energy cost of initiating a string — capturing the statistics of the smallest possible activation barriers. The derivative with respect to F^\ddagger converts from the cumulative probability that the free energy barrier is below F^\ddagger to the probability the free energy barrier is between F^\ddagger and $F^\ddagger + dF^\ddagger$. G can be calculated explicitly by solving the diffusion equation using the method of images. The result may be represented in closed form in terms of the Jacobi theta function, however we leave the sum explicit to more easily examine the asymptotics

$$G = \frac{e^{\frac{\phi}{\delta f^2}(F - F_{\text{in}} - \phi N/2)}}{\sqrt{2\pi\delta f^2 N}} \times \sum_{n=-\infty}^{\infty} \left[e^{-\frac{(2nF^\ddagger + F - F_{\text{in}})^2}{2\delta f^2 N}} - e^{-\frac{(2nF^\ddagger + F + F_{\text{in}})^2}{2\delta f^2 N}} \right] \quad (5)$$

In the integral of equation 4 the cutoff N_{max} reflects the maximum size to which a stringy reconfiguration event would typically grow before compact rearrangements dominate. We estimate this maximum length as $N_{\text{max}} \approx F_\alpha^\ddagger/\phi$, since certainly by that length the most important reconfiguration events would be compact. We can simplify by smoothing the cutoff so that the finite integral $\int_0^{N_{\text{max}}} dN$ is replaced by $\int_0^\infty dN \exp(-N/N_{\text{max}})$. The smoothed distribution of free energy barriers follows directly from equations 4 and 5

$$\Gamma = \frac{\partial}{\partial F^\ddagger} \left\langle \exp \left(-\frac{F_{\text{in}}\phi}{\delta f^2} - \frac{1}{2}F_{\text{in}}q \right) \times \left(1 - \frac{\exp(F_{\text{in}}q) - 1}{\exp(F^\ddagger q) - 1} \right) \right\rangle_{0 < F_{\text{in}} < F^\ddagger} \quad (6)$$

where, $q \equiv \frac{2}{\delta f} \sqrt{\frac{2\phi}{F_\alpha^\ddagger} + \frac{\phi^2}{\delta f^2}}$

The result involves nothing more complicated than exponentials and error functions.

The total magnitude of the secondary relaxation peak is estimated by calculating the probability that fluctuations can stabilize a stringy reconfiguration for any size barrier less than F_α^\ddagger . Integrating Γ over F^\ddagger yields

$$\Psi \approx \exp \left\{ -\frac{2\phi(F_{\text{in}} - \phi)}{\delta f^2} \right\} \quad (7)$$

Ψ increases with temperature as the dynamical crossover at T_{string} is approached, a trend that is validated experimentally[25]. At the crossover temperature and above, this secondary relaxation becomes the only remaining mode of activated relaxation. The sharp transition from activated to non-activated motions at T_c that is predicted by the non-fluctuating RFOT theory, as well as by mode coupling theory[26, 27] and the mean field theory of supercooled liquids[28, 29, 30], is therefore smoothed out by the string-like activated events made possible by fluctuations and exhibits no divergent critical behavior at s_c^{string} [21]. In this temperature regime the secondary beta relaxations of mode coupling theory would be present and overlap in frequency with the string-like activated secondary relaxations, perhaps making the differentiation of the processes difficult.

Γ can be approximated by the Gumbel extreme value distribution function[31]. For $F^\ddagger > F_{\text{in}}$ the barrier distribution decays exponentially as

$$\Gamma(F^\ddagger > F_{\text{in}}) \sim \exp(-F^\ddagger q) \approx \exp \left(-2\frac{F^\ddagger \phi}{\delta f^2} \right) \quad (8)$$

The results agree with the sampled distribution of barriers for the string-like reconfiguration events alone (shown in figure 5). Using the fact that $\tau = \tau_0 \exp(F^\ddagger/k_B T)$ equation 8 gives a power law distribution of relaxation times $P(\tau) \sim \tau^{-\gamma}$ where $\gamma \approx 2(s_c^{\text{string}} - s_c)/\Delta C_P + 1$. Well above T_g the high barrier side of the secondary relaxation blends in with the primary relaxation peak. Thus the secondary relaxation from ramified reconfiguration events often appears as only a “wing” on the main distribution[32, 33].

In the aging glass, the picture of secondary relaxation is slightly modified. If the liquid fell out of equilibrium at T_f then the frozen-in structure has an average excess energy per particle $\epsilon(T_f) = \epsilon(T_K) + \int_{T_K}^{T_f} dT \Delta C_P(T)$. At temperatures $T < T_f$ a region of the liquid undergoing reconfiguration would relax to a structure with average energy $\epsilon(T) < \epsilon(T_f)$. Thus the driving force for reconfiguration gains an energetic contribution and the configuration entropy in equation 1 is replaced by $Ts_c \rightarrow (Ts_c + \Delta\epsilon)$ where $\Delta\epsilon = \epsilon(T_f) - \epsilon(T) = \int_T^{T_f} dT' \Delta C_P(T')$. Lubchenko and Wolynes[11] have shown that this additional driving force results in a change in slope of the typical relaxation time as a function of temperature, and a transition to nearly Arrhenius behavior as the system falls out of equilibrium. Correspondingly, falling out of equilibrium causes the string tension to be reduced by an amount $\Delta\epsilon$, giving $\phi = Ts_c^{\text{string}} - Ts_c - \Delta\epsilon$ and making the system appear closer to the dynamical crossover than an equilibrated system at the same temperature. Furthermore, the driving force fluctuations are frozen in as the aging glass falls out of equilibrium becoming largely independent of temperature. These changes broaden and flatten the barrier distribution as the temperature is lowered, giving

$$\Gamma(F^\ddagger > F_{\text{in}}) \sim \exp \left(-2\frac{F^\ddagger(Ts_c^{\text{string}} - Ts_c - \Delta\epsilon)}{T_f^2 k_B \Delta C_P(T_f)} \right) \quad (9)$$

for large F^\ddagger . The secondary relaxation strength in the aging regime becomes

$$\Psi \approx \exp \left\{ -\frac{2(Ts_c^{\text{string}} - Ts_c - \Delta\epsilon)}{T_f^2 k_B \Delta C_P(T_f)} \times (F_{\text{in}} - (Ts_c^{\text{string}} - Ts_c - \Delta\epsilon)) \right\}. \quad (10)$$

In the limit $T \rightarrow 0$ the distribution of barriers becomes largely independent of temperature with $\Gamma(F^\ddagger > F_{\text{in}}) \sim \exp(-\alpha F^\ddagger)$ and $\alpha \approx ((z - 2)v_{\text{int}}(T_f) -$

$\Delta\epsilon)/(T_f k_B \Delta C_P(T_f))$. For a broad enough distribution of barriers the dielectric absorption spectrum is determined through the simple relation, $\epsilon''(\omega) \sim P(F^\ddagger = -k_B T \ln \omega/\omega_0) \sim \omega^{\alpha T}$, and becomes flat for low temperatures, resembling the so called constant loss spectrum. In a rejuvenating glass, an aged system that is heated to a temperature above T_f , the energetic contribution to the driving force is negative, $\Delta\epsilon < 0$. In this situation the system appears as if it is further from the dynamical crossover temperature than an equilibrated system at the same temperature and secondary relaxations are relatively suppressed.

Nearly all glass forming liquids display, dynamical modes seemingly distinct from the primary alpha relaxations. We have shown that by adding fluctuations to the existing structure of random first order transition theory a tail develops on the low free energy side of the activation barrier distribution which shares many of the observed features of the secondary relaxations. The relaxation process responsible for the tail differs from the primary relaxation mechanism in the geometry of the region undergoing cooperative reconfiguration. While primary relaxation takes place through activated events involving compact regions, secondary relaxation is governed by more ramified string-like, or percolation-like clusters of particles. While the existence of secondary relaxation is nearly universal, the relevant motions are of shorter length scales than those for primary relaxation, allowing additional material dependent effects and, perhaps, less universal quantitative description than for the main relaxation. The present theory, however, suggests a universal mechanism for secondary relaxation. The theory points out some general trends about the way these relaxations vary with temperature and substance which conform to observation.

Support from NSF grant CHE0317017 and NIH grant 5R01GM44557 is gratefully acknowledged. Encouraging discussion on this topic with Vas Lubchenko, Hans Frauenfelder and Jörg Schmalian are gratefully acknowledged

-
- [1] Adichtchev, S. *et al.* Fast relaxation processes in glasses as revealed by depolarized light scattering. *Journal of Non-Crystalline Solids* **353**, 1491–1500 (2007).
 - [2] Kudlik, A., Benkhof, S., Blochowicz, T., Tschirwitz, C. & Rossler, E. The dielectric response of simple organic glass formers. *J. Mol. Struct.* **479**, 201–218 (1999).
 - [3] Ngai, K. L. & Capaccioli, S. Relation between the activation energy of the Johari-Goldstein β relaxation and T_g of glass formers. *Phys. Rev. E* **69**, 031501 (2004).
 - [4] Wang, L. M. & Richert, R. Primary and secondary relaxation time dispersions in fragile supercooled liquids. *Phys. Rev. B* **76**, 064201 (2007).
 - [5] Lunkenheimer, P., Schneider, U., Brand, R. & Loidl, A. Glassy dynamics. *Contemporary Phys.* **41**, 15–36 (2000).
 - [6] Frauenfelder, H. *et al.* A unified model of protein dynamics. *Proc. Natl. Acad. Sci. U.S.A.* (2009).
 - [7] Thayyil, M. S., Capaccioli, S., Prevosto, D. & Ngai, K. L. Is the Johari-Goldstein beta-relaxation universal? *Philosophical Magazine* **88**, 4007–4013 (2008).
 - [8] Lubchenko, V. & Wolynes, P. G. Theory of structural glasses and supercooled liquids. *Ann. Rev. Phys. Chem.* **58**, 235–266 (2007).
 - [9] Xia, X. & Wolynes, P. G. Fragilities of liquids predicted from the random first order transition theory of glasses. *Proc. Natl. Acad. Sci. U.S.A.* **97**, 2990–2994 (2000).
 - [10] Stevenson, J. D. & Wolynes, P. G. Thermodynamic-kinetic correlations in supercooled liquids: A critical survey of experimental data and predictions of the random first-order transition theory of glasses. *J. Phys. Chem. B* **109**, 15093–15097 (2005).
 - [11] Lubchenko, V. & Wolynes, P. G. Theory of aging in structural glasses. *J. Chem. Phys.* **121**, 2852–2865 (2004).
 - [12] Xia, X. & Wolynes, P. G. Microscopic theory of heterogeneity and nonexponential relaxations in supercooled liquids. *Phys. Rev. Lett.* **86**, 5526–5529 (2001).
 - [13] Dzero, M., Schmalian, J. & Wolynes, P. G. Replica theory for fluctuations of the activation barriers in glassy systems. *arXiv:0809.3988v1* (2008).
 - [14] Stevenson, J. D., Schmalian, J. & Wolynes, P. G. The shapes of cooperatively rearranging regions in glass-forming liquids. *Nature Phys.* **2**, 268–274 (2006).
 - [15] Kirkpatrick, T. R., Thirumalai, D. & Wolynes, P. G. Scaling concepts for the dynamics of viscous liquids near an ideal glassy state. *Phys. Rev. A* **40**, 1045–1054 (1989).
 - [16] Biroli, G., Bouchaud, J.-P., Cavagna, A., Grigera, T. S. & Verrocchio, P. Thermodynamic signature of growing amorphous order in glass-forming liquids. *Nature Phys.* **4**, 771–775 (2008).
 - [17] Cammarota, C., Cavagna, A., Gradenigo, G., Grigera, T. S. & Verrocchio, P. Surface tension fluctuations and a new spinodal point in glass-forming liquids. *arXiv* (2009). 0904.1522.
 - [18] Capaccioli, S., Ruocco, G. & Zamponi, F. Dynamically correlated regions and configurational entropy in supercooled liquids. *J. Phys. Chem. B* **112**, 10652–10658 (2008).
 - [19] Stevenson, J. D., Walczak, A. M., Hall, R. W. & Wolynes, P. G. Constructing explicit magnetic analogies for the dynamics of glass forming liquids. *J. Chem. Phys.* **129**, 194505 (2008).
 - [20] Adam, G. & Gibbs, J. H. On the temperature dependence of cooperative relaxation properties in glass-forming liquids. *J. Chem. Phys.* **43**, 139–146 (1965).
 - [21] Bhattacharyya, S. M., Bagchi, B. & Wolynes, P. G. Facilitation, complexity growth, mode coupling, and activated dynamics in supercooled liquids. *Proc. Natl. Acad. Sci. U.S.A.* **105**, 16077–16082 (2008).
 - [22] Flory, P. J. *Principles of Polymer Chemistry* (Cornell University Press Ltd., 1953).
 - [23] Hagedorn, R. Statistical thermodynamics of strong interactions at high-energies. *Nuovo Cim. Suppl.* **3**, 147 (1965).
 - [24] Plotkin, S. S. & Wolynes, P. G. Buffed energy landscapes: Another solution to the kinetic paradoxes of protein folding. *Proc. Natl. Acad. Sci. U.S.A.* **100**, 4417–4422 (2003).

- [25] Wiedersich, J. *et al.* Fast and slow relaxation processes in glasses. *J. Phys.: Cond. Matt.* **11**, A147–A156 (1999).
- [26] Leutheusser, E. Dynamical model of the liquid-glass transition. *Phys. Rev. A* **29**, 2765–2773 (1984).
- [27] Gotze, W. & Sjogren, L. Relaxation processes in supercooled liquids. *Reports On Progress In Phys.* **55**, 241–376 (1992).
- [28] Singh, Y., Stoessel, J. P. & Wolynes, P. G. Hard-sphere glass and the density-functional theory of aperiodic crystals. *Phys. Rev. Lett.* **54**, 1059–1062 (1985).
- [29] Franz, S. Metastable states, relaxation times and free-energy barriers in finite-dimensional glassy systems. *Europhys. Lett.* **73**, 492–498 (2006).
- [30] Mezard, M. & Parisi, G. Statistical physics of structural glasses. *J. Phys.: Cond. Matt.* **12**, 6655–6673 (2000).
- [31] Bertin, E. Global fluctuations and gumbel statistics. *Phys. Rev. Lett.* **95**, 170601 (2005).
- [32] Blochowicz, T., Tschirwitz, C., Benkhof, S. & Rossler, E. A. Susceptibility functions for slow relaxation processes in supercooled liquids and the search for universal relaxation patterns. *J. Chem. Phys.* **118**, 7544–7555 (2003).
- [33] Blochowicz, T., Gainaru, C., Medick, P., Tschirwitz, C. & Rossler, E. A. The dynamic susceptibility in glass forming molecular liquids: The search for universal relaxation patterns II. *J. Chem. Phys.* **124**, 134503 (2006).